ARTICLE IN PRESS

Neurobiology of Aging xxx (2015) 1–10

Contents lists available at ScienceDirect

Neurobiology of Aging

journal homepage: www.elsevier.com/locate/neuaging

FK506 reduces neuroinflammation and dopaminergic neurodegeneration in an α-synuclein-based rat model for Parkinson's disease

Anke Van der Perren [a], Francesca Macchi [a], Jaan Toelen [b], Marianne S. Carlon [b], Michael Maris [b], Henriette de Loor [c], Dirk R.J. Kuypers [c], Rik Gijsbers [b,d], Chris Van den Haute [a,d], Zeger Debyser [b,d], Veerle Baekelandt [a,d,*]

[a] *Laboratory for Neurobiology and Gene Therapy, Department of Neurosciences, KU Leuven, Flanders, Belgium*
[b] *Molecular Virology and Gene Therapy, Department of Pharmaceutical and Pharmacological Sciences, KU Leuven, Flanders, Belgium*
[c] *Division of Nephrology and Renal Transplantation, Department of Microbiology and Immunology, Leuven University Hospital and KU Leuven, Leuven, Belgium*
[d] *Leuven Viral Vector Core, KU Leuven, Leuven, Belgium*

ARTICLE INFO

Article history:
Accepted 25 November 2014

Keywords:
α-Synuclein
Parkinson's disease
FK506
Neuroinflammation
Microglia

ABSTRACT

Alpha-synuclein (α-synuclein) is considered a key player in Parkinson's disease (PD), but the exact relationship between α-synuclein aggregation and dopaminergic neurodegeneration remains unresolved. There is increasing evidence that neuroinflammatory processes are closely linked to dopaminergic cell death, but whether the inflammatory process is causally involved in PD or rather reflects secondary consequences of nigrostriatal pathway injury is still under debate. We evaluated the therapeutic effect of the immunophilin ligand FK506 in a rAAV2/7 α-synuclein overexpression rat model. Treatment with FK506 significantly increased the survival of dopaminergic neurons in a dose-dependent manner. No reduction in α-synuclein aggregation was apparent in this time window, but FK506 significantly lowered the infiltration of both T helper and cytotoxic T cells and the number and subtype of microglia and macrophages. These data suggest that the anti-inflammatory properties of FK506 decrease neurodegeneration in this α-synuclein-based PD model, pointing to a causal role of neuroinflammation in the pathogenesis of PD.

1. Introduction

Parkinson's disease (PD) is a slowly progressing movement disorder and is characterized by a progressive loss of dopaminergic neurons (DN) in the substantia nigra pars compacta (SNpc) along with the accumulation of aggregated forms of the protein α-synuclein in nigral neurons as well as in other brain regions. The loss of dopaminergic innervation leads to depletion of striatal dopamine, resulting in the progressive decline of movement control (Ma et al., 1997). Currently, most treatments of PD are focused on the symptomatic improvement of motor symptoms related to the loss of the DN in the SNpc. These symptomatic treatments significantly improve quality of life and life expectancy. Still, the development of therapeutic approaches that slow or halt the disease progression remains crucial. Mounting evidence suggests that both innate and adaptive immune responses could contribute to dopaminergic neurodegeneration and are potentially linked to disease progression (Braak et al., 2007). However, the contribution of the different subsets of immune cells and the trigger by which these cells get activated is still very unclear.

FK506, also named tacrolimus, has been proposed to exert neuroprotective and neuroregenerative effects in animal models of PD (Gold and Nutt, 2002; Poulter et al., 2004). Administration of FK506 has previously been described to reduce dopamine depletion in the striatum of 1-methyl- 4 phenyl-1,2,3,6-tetrahydropyridine-treated mice (Kitamura et al., 1994) and to delay ibotenic acid-induced neurodegeneration in the globus pallidus of rats (Wright et al., 2008). We have demonstrated that inhibition by FK506 reduces α-synuclein aggregation and associated neuronal cell death in cell culture and in a mouse PD model (Gerard et al., 2010).

FK506 is a well-known immunosuppressive drug that is mainly used posttransplantation to decrease the activity of the recipient's immunity. The effects of FK506 within the immune system are well

* Corresponding author at: Laboratory for Neurobiology and Gene Therapy, Department of Neurosciences, KU Leuven, Kapucijnenvoer 33—VCTB+5, B-3000 Leuven, Flanders, Belgium. Tel.: +32 16 33 21 94; fax: +32 16 33 63 36.
E-mail address: Veerle.Baekelandt@med.kuleuven.be (V. Baekelandt).

0197-4580/$ – see front matter © 2015 Elsevier Inc. All rights reserved.
http://dx.doi.org/10.1016/j.neurobiolaging.2015.01.014

characterized. FK506 binds to the immunophilin FKBP (FK506-binding protein). The FK506-FKBP complex interacts with and inhibits calcineurin, a calcium- and calmodulin-dependent phosphatase, resulting in both the suppression of a T-lymphocyte signal transduction pathway and IL2 transcription (Liu et al., 1991, 1992). The mode of action for its neuroprotective effects remains to be elucidated. Different types of action have been described to FK506, inhibition of apoptosis and necrosis, attenuation of leukocyte accumulation, and reduction of microglia activation. In addition, our group has showed a direct link between FKBP12 and α-synuclein aggregation (Deleersnijder et al., 2011; Gerard et al., 2008, 2010).

We developed a robust rat model for PD by injection of adeno-associated viral vectors (rAAV2/7)–encoding α-synuclein into the substantia nigra (SN) resulting in reproducible nigrostriatal pathology (Van der Perren et al., 2014). This α-synuclein rat model shows improved face and predictive validity. It therefore offers new opportunities for both preclinical testing of potential treatments and understanding the disease mechanism.

In this study, we evaluated the therapeutic effect of FK506 and the role of neuroinflammation in α-synuclein–induced neurodegeneration. Treatment with FK506 significantly increased the survival of DN in a dose-dependent way. No reduction in α-synuclein aggregation was apparent in this time window, but FK506 significantly lowered the infiltration of both T helper and cytotoxic T cells and the number of microglia and macrophages. These data suggest that the anti-inflammatory properties of FK506 decrease the level of neurodegeneration in this α-synuclein-based PD model, pointing to a causal role of neuroinflammation in the pathogenesis of PD.

2. Methods

2.1. Recombinant AAV production and purification

Vector production and purification was performed as previously described (Van der Perren et al., 2011). The plasmids include the constructs for the AAV2/7 serotype, the AAV transfer plasmid encoding the human A53T α-synuclein mutant, or eGFP as a control under the control of the ubiquitous CMVie–enhanced synapsin1 promoter and the pAdvDeltaF6 adenoviral helper plasmid. Real-time polymerase chain reaction analysis was used for genomic copy determination.

2.2. Stereotactic injections

All animal experiments were carried out in accordance with the European Communities Council Directive of 24 November, 1986 (86/609/EEC) and approved by the Bioethical Committee of the KU Leuven (Belgium). Young, adult, female Wistar rats (Janvier, France) weighing about 200–250 g were housed under a normal 12 -hour light and dark cycle with free access to pelleted food and tap water. All surgical procedures were performed using aseptic techniques and ketamine (60 mg/kg i.p., Ketalar, Pfizer, Belgium) and medetomidine (0.4 mg/kg, Dormitor, Pfizer) anesthesia. After anesthesia, the rodents were placed in a stereotactic head frame (Stoelting, IL, USA). Injections were performed with a 30-gauge needle and a 10-μL Hamilton syringe. All animals were injected with 3 μL rAAV2/7A53T α-synuclein or rAAV2/7 eGFP as a control (3.0 E + 11 GC/mL). Stereotactic coordinates used for the SN were anteroposterior −5.3, lateral −2.0, and dorsoventral −7.2, calculated from the dura using bregma as reference. The injection rate was 0.25 μL/min, the needle was left in place for an additional 5 minutes before being retracted.

2.3. Histology

Rats were sacrificed with an overdose of sodium pentobarbital (60 mg/kg, i.p., Nembutal, Ceva Santé, Belgium) followed by intracardial perfusion with 4% paraformaldehyde in phosphate buffered saline. After postfixation overnight, 50-μm-thick coronal brain sections were made with a vibrating microtome (HM 650V, Microm, Germany). Immunohistochemistry (IHC) was performed on free-floating sections using an antibody against α-synuclein (1:5000, Chemicon 5038). We also used antibodies against tyrosine hydroxylase (TH) (1:1000, Chemicon 152), Mac1 (CD11b, 1:500, Serotec), CD68 (1:500, Millipore), MHCII (1:250, Serotec), CD4 (1:500, Serotec), and CD8 (1:500, Serotec). Sections were pretreated with 3% hydrogen peroxide for 10 minutes and incubated overnight with primary antibody in 10% normal goat or swine serum (DakoCytomation, Belgium). As secondary antibody, we used biotinylated anti-rabbit IgG (1:600 [α-synuclein], 1:300 [other antibodies] DakoCytomation), followed by incubation with streptavidin–horseradish peroxidase complex (1:1000, DakoCytomation). α-Synuclein and Mac1, CD68, MHCII, and CD8 immunoreactivities were visualized using 3,3-diaminobenzidine (0.4 mg/mL, Sigma-Aldrich), and TH immunoreactivity was visualized using Vector SG (SK-4700, Vector Laboratories, CA) as a chromogen.

2.4. Scoring method

The levels of CD68 expression were scored 0–4. Score 0, no positive cells; score 1, few isolated positive cells; score 2, scattered cells; score 3, staining throughout the SNpc; score 4, staining throughout the whole SN. The levels of MHCII expression were scored 0–5. Score 0, no positive cells; score 1, few isolated positive cells; score 2, scattered cells; score 3, mild staining throughout the SNpc; score 4, extensive staining throughout the SNpc, score 5, extensive staining throughout the whole SN. All the analyses were performed by an investigator blind to treatment group.

2.5. Stereological quantification

The number of TH-positive cells and α-synuclein–positive cells in the SN was determined by stereological measurements using the Optical fractionator method in a computerized system as described previously (Baekelandt et al., 2002) (StereoInvestigator; MicroBrightField, Magdeburg, Germany). Every fifth section throughout the entire SN was analyzed, with a total of 7 sections for each animal. The coefficients of error, calculated according to the procedure of Schmitz and Hof as estimates of precision (Schmitz and Hof, 2005) varied between 0.05 and 0.10. We quantified both the injected and noninjected SN (internal control); no cell loss was observed in the noninjected side. The number of CD4- and CD8-positive T cells was determined using the Optical fractionator method. The percentage of Mac1-positive area was defined by densitometry using Image J software. The different types of Mac1 (CD11b)-positive microglia were quantified using stereological measurements and depicted as a percentage of the microglia sampled. All the analyses were performed by an investigator blind to different groups.

2.6. Behavioral testing

The cylinder test was used to quantify forelimb use. Contacts made by each forepaw with the wall of 20-cm-wide clear glass cylinder were scored from the videotapes by an observer blinded to the animal's identity. A total of 20 contacts were recorded for each animal. The number of impaired forelimb contacts was expressed as

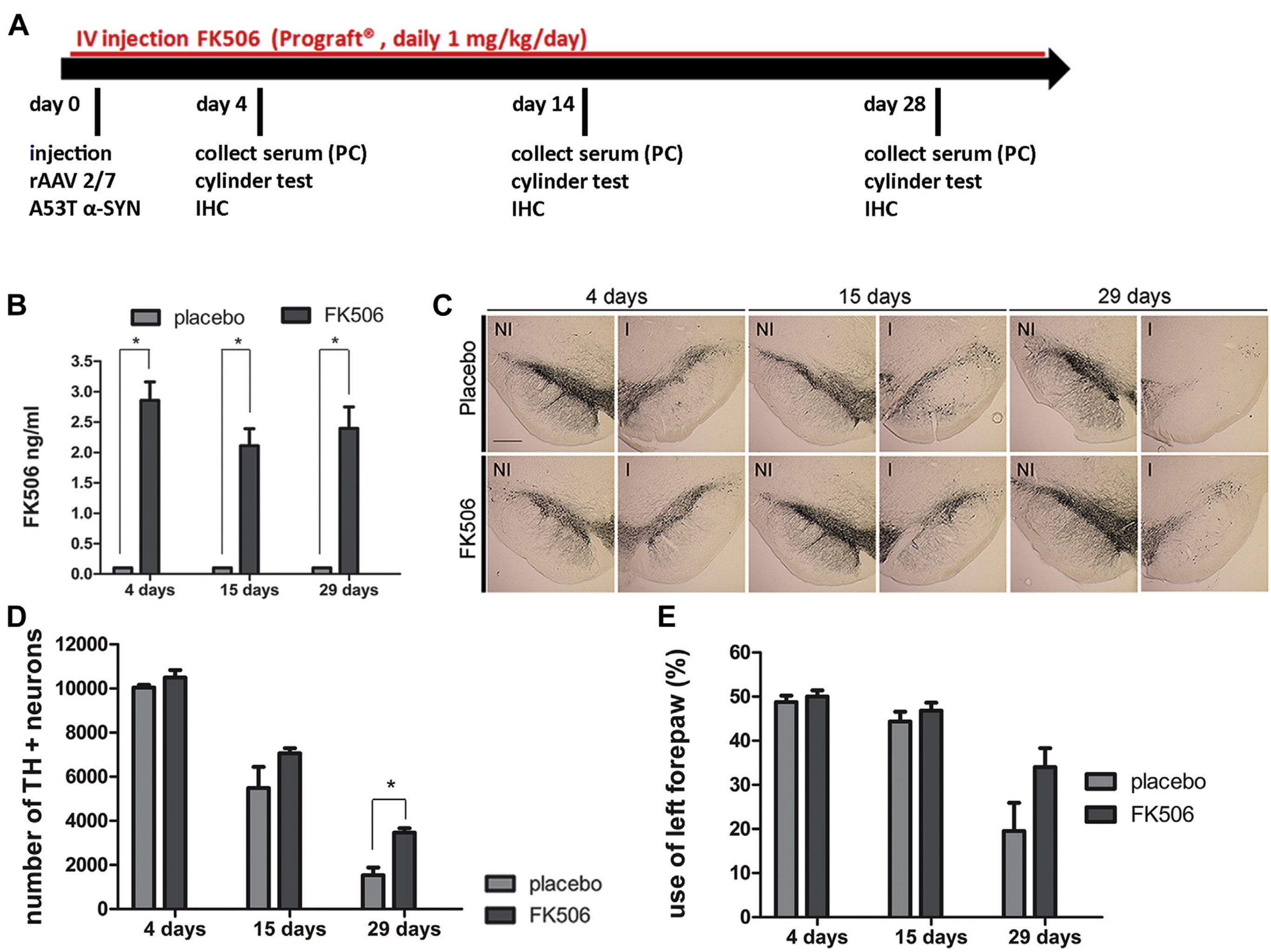

Fig. 1. FK506 reduces A53T α-synuclein induced neurodegeneration. (A) Schematic experimental presentation. (B) Measurement of FK506 whole-blood concentrations after daily systemic administration of FK506 (1 mg/kg) or placebo in A53T α-synuclein rAAV2/7-injected animals (standard vector dose) (mean ± SEM, $^*p < 0.05$ by ANOVA and Bonferroni post hoc test, n = 6–8). (C) IHC staining for TH in the SN over time after daily systemic administration of FK506 (1 mg/kg) or placebo in A53T α-synuclein rAAV2/7-injected animals. Scale bar = 500 μm. (D) Stereological quantification of the number of TH immunoreactive nigral neurons over time after daily systemic administration of FK506 (1 mg/kg) or placebo in A53T α-synuclein rAAV2/7-injected animals (mean ± SEM, $^*p < 0.05$ by ANOVA and Bonferroni post hoc test, n = 6). (E) Cylinder test at different time points after daily systemic administration of FK506 (1 mg/kg) or placebo in A53T α-synuclein rAAV2/7-injected animals (mean ± SEM, n = 6–8). Abbreviations: ANOVA, analysis of variance; SEM, standard error of the mean; SN, substantia nigra.

a percentage of total forelimb contacts. Nonlesioned control rats should score around 50% in this test.

2.7. *FK506 treatment: administration and measurement of FK506 concentrations in the blood and cerebrospinal fluid*

The FK506-treated animals were daily injected in the lateral tail vein with 1 mg/kg FK506 (Astellas amp. inf., stock conc. 5 mg/mL), starting 1 day after rAAV2/7 α-synuclein injection. The stock concentration was dissolved in saline to a work concentration of 0.25 mg/mL. For intravenous (IV) injection, the animals were anesthetized with isoflurane as described previously (Deroose et al., 2006). The placebo-treated animals were injected with the same solution as the FK506-treated animals without the active compound (10 mg/mL Cremophor RH60, 32 mg/mL EtOH in saline). To analyze the bioavailability and the presence of FK506 in the brain, a separate group of Wistar rats (n = 3–5) were injected IV for 3 days (to obtain steady-state concentrations) with different concentrations of FK506 (0.5, 1.0, 1.5, 2.0, and 3.0 mg/kg) (stock concentration 0.25 mg/mL for 0.5–1.0 and 1.5 mg/kg FK506 and 0.5 mg/mL for 2 and 3 mg/kg FK506). One hour after the last IV injection blood (tail vein) and cerebrospinal fluid (CSF) (cistern magna) samples were taken to determine peak values. The animals were injected for 5 more days and 24 hours after the last IV injection blood, and CSF samples were taken to determine trough values.

FK506 whole-blood concentrations were measured using a commercially available liquid chromatography tandem mass-spectrometry kit and validated according to National Committee for Clinical Laboratory Standards and Food and Drugs Administration (NCCLS and FDA) guidelines (MassTrak Immunosuppressants Kit, Waters, Zellik, Belgium) (Napoli et al., 2010). A description of this method was recently published (de Jonge et al., 2012). The samples were injected on an Alliance 2695 HPLC, and the detection was performed using a Quattro micro API tandem mass spectrometer (Waters) (for detailed information see Supplementary Fig. 1). Because of lower concentrations of FK506 in CSF samples, a second sample preparation and a higher sensitive mass spectrometry was needed. In brief, 50 μL zinc sulfate (0.1 M) was added to 50 μL CSF sample in a polypropylene tube (1.5 mL). After vortex mixing, 150 μL of internal standard solution (ascomycin dissolved in acetonitrile,

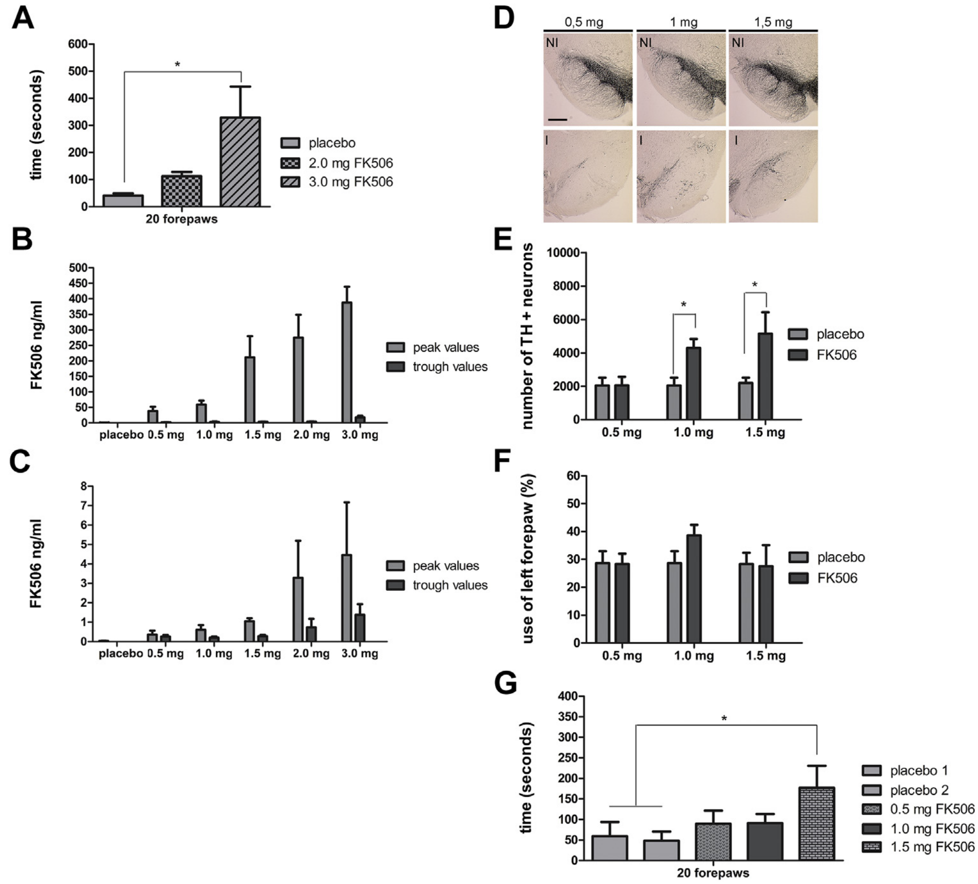

Fig. 2. Dose-dependent effects of FK506 in the A53T α-synuclein rAAV2/7 rat model. (A) Time necessary to place 20 forepaws in the cylinder test 29 days after administration of 2 and 3 mg/kg FK506 (Mean ± SEM, * $p < 0.05$ by ANOVA and Bonferroni post hoc test, n = 6–8). (B) Blood and (C) CSF levels of FK506 were determined 1 hour (peak) and 24 hours (trough) after administration in Wistar rats (mean ± SEM, n = 3–5). (D) IHC staining for TH in the SN after daily systemic administration of FK506 (0.5,1.0, and 1.5 mg/kg) or placebo in A53T α-synuclein rAAV2/7-injected animals. Scale bar = 500 µm. (E) Stereological quantification of the number of TH immunoreactive nigral neurons after systemic administration of different doses of FK506 (0.5, 1.0, and 1.5 mg/kg) or placebo for 29 days in A53T α-synuclein rAAV2/7-injected animals (mean ± SEM, *$p < 0.05$ by ANOVA and Bonferroni post hoc test, n = 6–8). (F) Cylinder test after systemic administration of different doses of FK506 or placebo for 29 days in A53T α-synuclein rAAV2/7-injected animals (mean ± SEM, n = 6–8). (G) Time necessary to place 20 forepaws in the cylinder test 29 days after administration of 0.5, 1.0, and 1.5 mg/kg FK506 (mean ± SEM, *$p < 0.05$ by ANOVA and Bonferroni post hoc test, n = 6–8). Abbreviations: ANOVA, analysis of variance; CSF, cerebrospinal fluid; SEM, standard error of the mean; SN, substantia nigra.

final ascomycin concentration 0.5 ng/mL) was added. The samples were vortex mixed for 20 seconds and centrifuged at 16,000*g*, 24 °C for 2 minutes. The supernatant was then transferred, and 20 µL was injected onto the Acquity UPLC with a high-end tandem mass spectrometry Xevo TQS (Waters). Chromatographic separation was performed on a Acquity UPLC BEH 300 C4 column (1.7 µm, 2.1 × 100 mm; Waters) with a flow rate of 0.6 mL/min. The mobile phase was a gradient with 2 mM ammonium acetate and 0.1% formic acid in both Milli-Q water (A) and methanol (B). The gradient was as follows: after an initial conditioning of 0.5 minutes of 50% B, the gradient increased to 100% B in 1 minute; then immediately returning over 1 minute to 50% B, and finally equilibrating at 50% B for 2 minutes before the next injection.

For both whole blood and CSF samples, the ionization was achieved using electrospray in the positive ionization mode, and the mass spectrometer was operated in multiple-reaction monitoring mode. The multiple-reaction monitoring transitions used for quantification were m/z 821→768 for FK506 and 809→756 for ascomycin. Analyte was quantified by use of peak area ratios of analyte over internal standard using non-weighted linear regression.

The quantification of whole-blood concentrations of FK506 was achieved by using the calibrators (covering a linear range from 0 to 30 ng/mL) and controls (low, medium, and high concentration) of the MassTrak Immunosuppressant kit. The analytical performance of the kit was validated by successful participation of our laboratory in the International Tacrolimus Proficiency Testing Scheme provided by Analytical Services International Ltd (London, UK). Calibration curves for the quantification of FK506 concentrations in CSF were prepared by spiking FK506 on artificial CSF (http://www.alzet.com/products/guide_to_use/cfs_preparation.html). The calibration curve was linear over the range of 0.075–20 ng/mL. The limit of detection and the lower limit of quantification were 0.05 and 0.15 ng/mL, respectively. The inter-assay (n = 5 in triplicate) and intra-assay (n = 4 in duplicate) were below 9%. The recovery of FK506 in rat CSF was 88% (n = 4).

3. Results

3.1. FK506 reduces A53T α-synuclein–induced neurodegeneration in vivo

Different neuroprotective and neuroregenerative properties have been attributed to immunophilin ligands such as FK506, but the exact mechanism remains unclear (Gold and Nutt, 2002; Poulter et al., 2004). Because we have previously implicated FKBP12 as a facilitator of α-synuclein aggregation and neurotoxicity (Deleersnijder et al., 2011; Gerard et al., 2010), we hypothesized that FK506 could reduce α-synuclein–induced dopaminergic neurodegeneration in our rat model. Therefore, we administered FK506 (1 mg/kg) daily for 4 weeks in the A53T α-synuclein rAAV2/7 rat model (Fig. 1A). As the bioavailability of FK506 by oral delivery can vary (Iwasaki, 2007), we administered FK506 IV. Liquid chromatography tandem mass-spectrometry confirmed elevated blood levels of FK506 at all time points (4 days, 2.86 ± 0.61 ng/mL; 15 days, 2.11 ± 0.69 ng/mL; and 29 days, 2.40 ± 0.93 ng/mL) compared with placebo-treated animals (Fig. 1B). All animals tolerated the daily IV injection of FK506 well, without obvious physical symptoms except for mild diarrhea. Quantification of the number of TH immunoreactive nigral neurons at 29 days post injection (p.i.) demonstrated a more than 2-fold higher survival of DN in the rats treated with FK506 compared with placebo controls (Fig 1C and D). To prove that we observed real neuronal death, we additionally performed a vesicular monoamine transporter 2 and a Nissl staining. Both indicated clear dopaminergic cell death in the SN (data not shown).

To assess the functional effect of the FK506 treatment, the rats were subjected to the cylinder test at 3 different time points (4 days, 15 days, and 29 days p.i.). We noted improvement in the FK506-treated group (34% ± 10%) compared with the placebo group (18% ± 16%), but this difference did not reach statistical significance (Fig. 1E).

Based on these results, we decided to perform a dose-response study to evaluate the therapeutic window of FK506. First, we tested a dose of 2 mg/kg and 3 mg/kg FK506 in A53T synuclein rAAV2/7–injected rats, but these higher doses of FK506 were not well tolerated. The animals displayed an overall decrease in spontaneous movements (Fig. 2A), severe weight loss over time, and increased mortality rates. Therefore, we decided to lower the range to 0.5–1.0 and 1.5 mg/kg FK506. Administration of these lower doses in A53T synuclein rAAV2/7–injected rats for 29 days was well tolerated. To test the bioavailability of FK506 in vivo and the presence of FK506 in the brain, we measured peak and trough levels in blood and CSF samples after treatment with the different doses of FK506 (Fig. 2B and C). These values were in line with the administered dose range with peak values in the blood between 38 and 388 ng/mL and in the CSF between 0.36 and 4.5 ng/mL. In rats that received 1.0 mg/kg FK506, the median ratio of 24 hours trough FK506 concentrations in blood to that in CSF was 10.70 (range: 6.8–57.1). For FK506 doses of 0.5 and 1.5 mg/kg, similar median blood-to-CSF concentration ratios were observed. Analysis of the number of surviving dopaminergic neurons revealed that animals treated with 1.0 mg/kg FK506 again displayed significant neuroprotection, confirming the results of the first experiment. Rats treated with 1.5 mg/kg FK506 also presented a significant higher dopaminergic cell survival compared with the placebo-treated animals, whereas no difference was seen in the 0.5 mg/kg treated-animals (Fig. 2D and E). In terms of motor behavior, again, rats that received 1.0 mg/kg FK506 showed a nonsignificant improvement in the use of the lesioned paw (39% ± 11%) compared with the placebo group (29% ± 12%), although, as expected, no differences were observed in the 0.5 mg/kg group. Interestingly, no behavioral improvement was observed in the animals treated with 1.5 mg/kg (Fig. 2F). Because of the generalized locomotor impairment observed in the animals treated with 2 and 3 mg/kg FK506, we also tested spontaneous movements in the lower-dose groups. This revealed that the 1.5 mg/kg FK506 group was considerably slower in forepaw use, which might explain the negative results in the cylinder test (Fig. 2G).

3.2. FK506 does not significantly affect A53T α-synuclein aggregation within 1 month time frame

To understand the mechanism by which FK506 prevents α-synuclein–induced degeneration, we first investigated whether FK506 affects α-synuclein aggregation in the brain. As 1 mg/kg

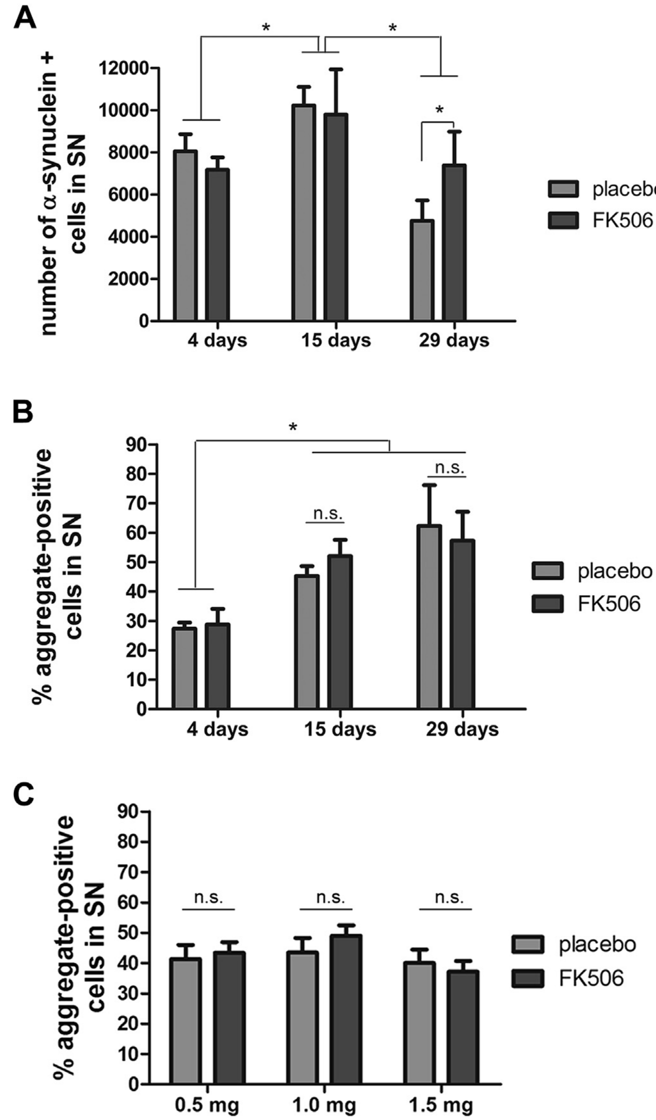

Fig. 3. FK506 does not modulate α-synuclein aggregation within 1 month time frame. (A) Stereological quantification of the number of α-synuclein–positive nigral cells after FK506 (1 mg/kg) treatment (mean ± SD, $^*p < 0.05$ by ANOVA and Bonferroni post hoc test, n = 6). (B) The percentage of aggregate-positive cells in the SN over time after FK506 (1 mg/kg) treatment (mean ± SD, $^*p < 0.05$ by ANOVA and Bonferroni post hoc test, n = 6). (C) The percentage of aggregate-positive cells in the SN 29 days after FK506 (0.5, 1.0, and 1.5 mg/kg) treatment (mean ± SD, $^*p < 0.05$ by ANOVA and Bonferroni post hoc test, n = 6). Abbreviations: ANOVA, analysis of variance; SD, standard deviation; SN, substantia nigra.

FK506 seemed to be the most effective dose, more detailed analysis was first performed in this cohort. Quantification of the total number of α-synuclein–positive cells in the SN revealed a significant increase in the animals treated with 1 mg/kg FK506 29 days after injection compared with the placebo–treated animals, consistent with the increased survival of dopaminergic neurons (Fig. 3A). When we divided the α-synuclein–positive cells into those with and without aggregates, no differences were observed in the ratio of aggregate-positive to aggregate-negative cells (Fig. 3B). When we evaluated animals treated with a higher (1.5 mg/kg) or lower dose of FK506 (0.5 mg/kg), also no difference in the ratio of aggregate-positive to aggregate-negative cells was detected (Fig. 3C). As FK506 did not seem to have an effect via α-synuclein aggregation, we hypothesized that the responsible mechanism was an effect on inflammation.

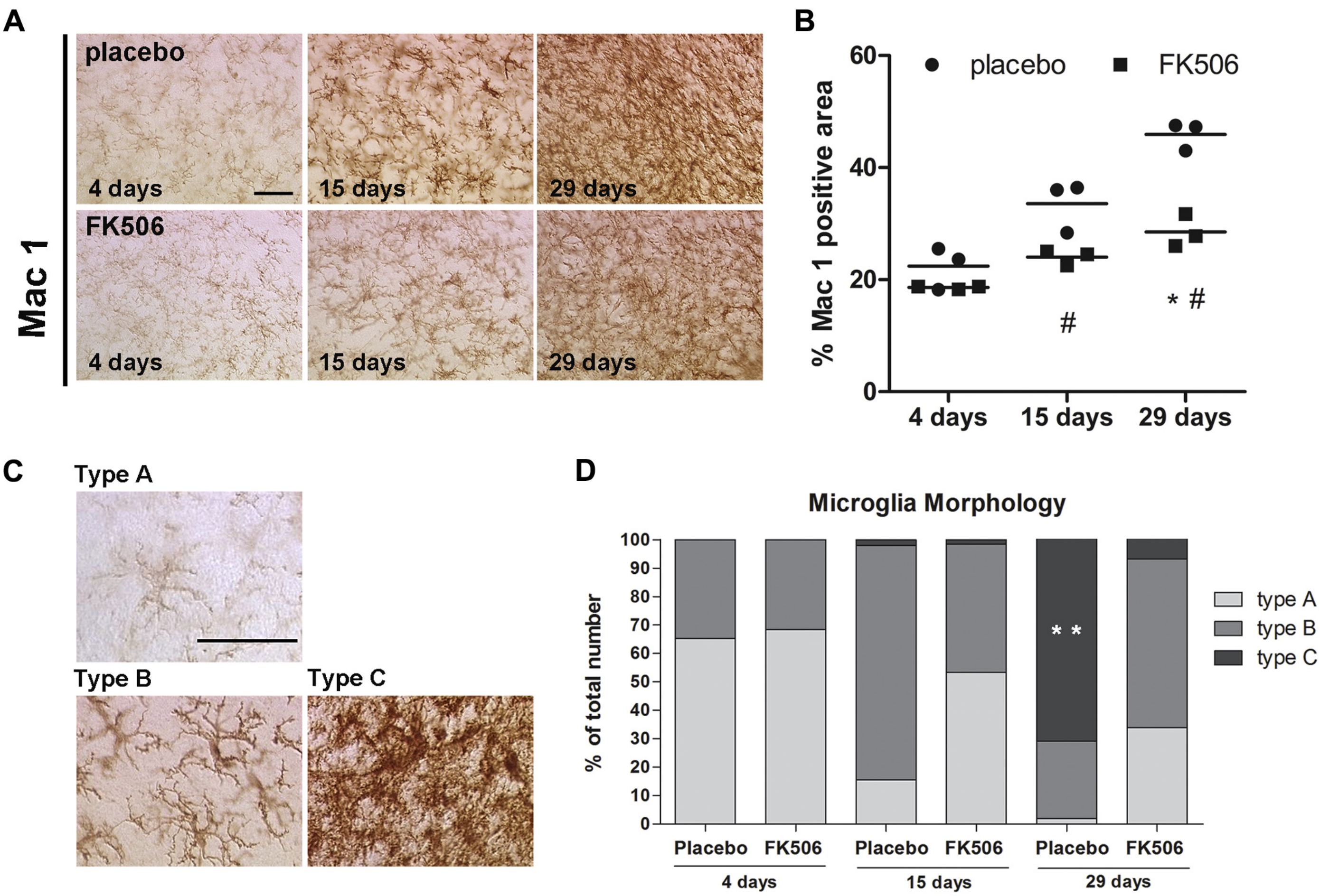

Fig. 4. FK506 reduces the number of A53T α-synuclein induced microglia and macrophages in vivo. (A) IHC staining for Mac1 demonstrating the presence of microglia at different time points after injection of A53T α-synuclein rAAV2/7 (standard vector dose) with daily placebo or FK506 treatment (1 mg/kg). Scale bar = 50 μm. (B) Quantification of the percentage of Mac1-positive area using Image J (mean ± SD, $^{*}p < 0.05$ vs. 4 days for both groups, $\#p < 0.05$ vs. the placebo-treated animals by ANOVA and Tukey post hoc test, n = 3). (C) The 3 morphologies of microglia are represented: type A (resting microglia), type B (isolated microglia), and type C (microglia in clusters). Scale bar = 70 μm. (D) Quantification of each morphology type is depicted as the average percentage distribution per group as a function of time (mean, $^{**}p < 0.01$ to the other group at same time point by 2-way ANOVA and Tukey post hoc test, n = 3). Abbreviations: ANOVA, analysis of variance; SD, standard deviation.

3.3. FK506 attenuates neuroinflammation

As FK506 also has strong immunosuppressive and anti-inflammatory properties (Kaminska et al., 2004), we decided to analyze the local microglia population in our A53T α-synuclein rAAV2/7 rat model. The microglial cells in the injected SN were visualized by Mac1 (CD11 b) staining, which detects all microglia and macrophages present (proinflammatory, anti-inflammatory, infiltrated macrophages, and proliferated microglia). The number of Mac1-positive microglia and macrophages increased in both groups over time (Fig. 4A), but FK506-treated rats showed significantly less Mac1-positive cells compared with placebo controls at 15 and 29 days postinjection (Fig. 4B). Only few microglia were detected in control animals injected with rAAV2/7eGFP and in the contralateral SN of all rats (Supplementary Fig. 1A).

In addition, we subdivided the microglia into 3 subtypes (Sanchez-Guajardo et al., 2010): type A cells "resting" microglia, type B cells "isolated activated microglia", type C microglial cells "tendency to form clusters" (Fig. 4C). We detected a predominance of type A microglia in placebo- and FK506-treated animals 4 days p.i. At 15 days p.i., we observed an increase in the percentage of type B microglia in both groups, but this increase was less pronounced in the FK506-treated animals. At 29 days p.i., type C microglia were predominantly present in the placebo group and significantly more abundant than in FK506-treated animals (Fig. 4D).

To correlate morphology to function, we analyzed the expression levels of CD68 as a marker of phagocytic microglia and macrophages and MHC II for antigen presentation. The presence of CD68- and MHC II-positive cells was assessed by scoring between 1 and 5 (see Section 2) (Fig. 5A and B). Both markers were almost undetectable in naive animals. We observed an increase in CD68- and MHC II-positive microglia over time in both placebo- and FK506-treated rats, but no significant differences were detected between the groups (Fig. 5C). Control animals injected with eGFP rAAV2/7 showed a similar infiltration of CD68- and MHC II-positive microglia compared with A53T α-synuclein rAAV2/7-injected rats at day 4, but no increase was observed over time (Supplementary Fig. 1B and C).

Because the upregulation of MHC II in a subset of microglia suggests a possible role of the adaptive immune system, we investigated T-cell infiltration into the SN (Fig. 6). The number of CD4-positive cells significantly increased in both groups over time, but FK506-treated rats showed significantly less CD4-positive cells compared with placebo controls at 29 days p.i. (Fig. 6A–C). Furthermore, we detected a delayed infiltration of CD8-positive T cells in FK506-treated rats, reaching a maximum at 29 days p.i., compared with the placebo-treated animals which showed a peak

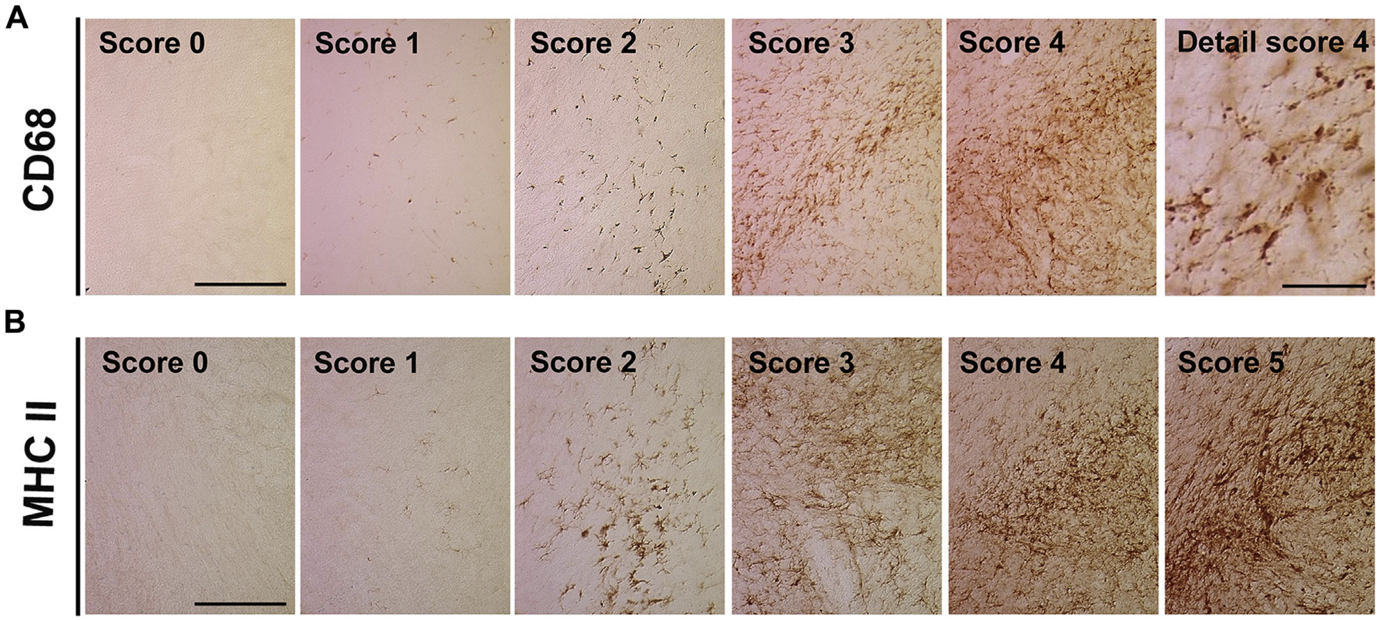

C

	4 days	15 days	29 days	
CD68				
placebo	**1.33 ± 0.58**	**3.00 ± 0.50 ***	**4.00 ± 0.00 #**	n.s.
FK506	**1.67 ± 0.58**	**3.17 ± 0.29 ***	**3.83 ± 0.29 #**	
MHCII				
placebo	**1.00 ± 0.00**	**2.00 ± 0.87 ***	**5,00 ± 0,76 #**	n.s.
FK506	**1.00 ± 0.00**	**2.83 ± 0.76 ***	**4.17 ± 0.29 #**	

Fig. 5. FK506 does not affect the number of CD68+ and MHC II+ cells. (A) The levels of CD68 expression were given a score of 0–4. Scale bar = 200 μm. (B) The levels of MHCII expression were given a score of 0–5. Scale bar = 200 μm. (C) An observer blind to the sections identity scored expression levels based on number of positive cells and area covered, as explained in the Section 2 (mean ± SD, $^*p < 0.05$ vs. 4 days, $\#p < 0.05$ vs. 15 days by ANOVA and Tukey post hoc test, n.s. not significant, n = 3). Abbreviations: ANOVA, analysis of variance; SD, standard deviation.

infiltration of CD8-positive cells at 15 days p.i. (Fig. 6D–F). eGFP rAAV2/7–injected control rats were characterized by a mild CD8 infiltration at 4 days that disappeared over time (Supplementary Fig. 1D).

4. Discussion

In the present study, we show that FK506 reduces neurodegeneration in an improved rAAV2/7-mediated α-synuclein rat model for PD. Our data reveal that the neuroprotective effect of FK506 observed in our α-synuclein model, presumably results from reduced α-synuclein–induced neuroinflammation and hints to an important role of the immune response and neuroinflammation in dopaminergic neurodegeneration.

Our rAAV2/7 A53T α-synuclein rat model offers new opportunities for preclinical testing of potential treatments because progressive neurodegeneration, motor impairments, and α-synucleinopathy are present. In this study, we questioned whether FK506 could protect against α-synuclein–induced neurodegeneration in this rat model. Administration of FK506 has previously been described to reduce dopaminergic depletion in the striatum of 1-methyl- 4 phenyl-1,2,3,6-tetrahydropyridine-treated mice (Kitamura et al., 1994) and to delay ibotenic acid–induced neurodegeneration in the globus pallidus of rats (Wright et al., 2008).

In our rat model, the survival rate of DN was significantly higher in rats treated with FK506 (1 mg/kg) compared with placebo controls 4 weeks after A53T α-synuclein rAAV2/7 injection. Moreover, this neuroprotection resulted in a positive trend toward behavioral improvement. Taking into account the fast progression of neurodegeneration in our rat model, this 2-fold higher survival of DN is substantial. Lowering the dose of FK506 to 0.5 mg/kg abolished the neuroprotective effect, whereas increasing the dose to 1.5 mg/kg resulted in a higher survival of the dopaminergic neurons. However, higher doses (2–3 mg/kg) were not well tolerated and even 1.5 mg/kg already affected the general locomotor activity of the animals observed in the cylinder test, suggesting a small therapeutic

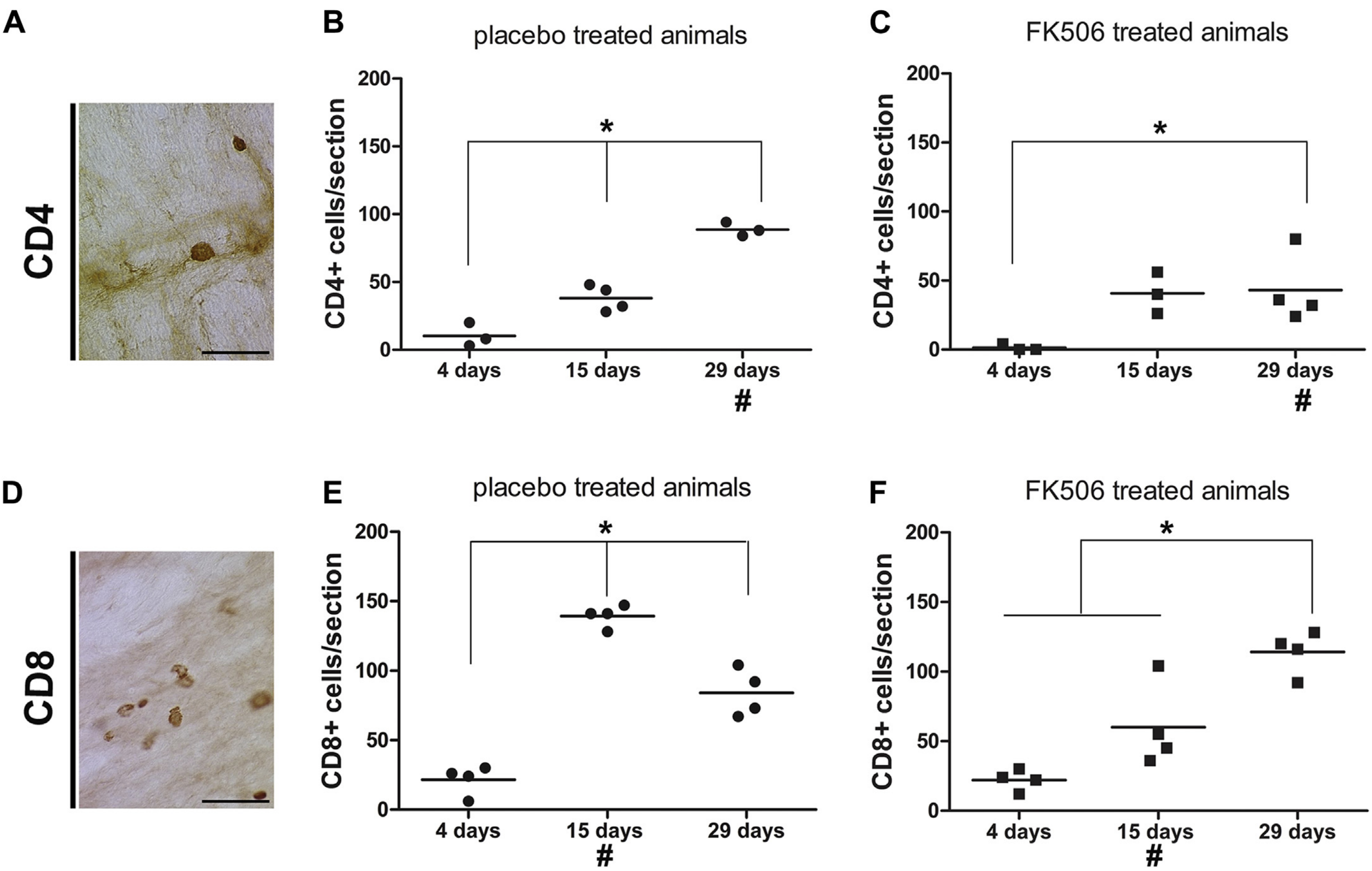

Fig. 6. FK506 reduces or delays the infiltration of CD4 and CD8+ T cells. (A) IHC staining for CD4 on placebo-treated animals 15 days after rAAV α-synuclein injection. Scale bar = 30 μm. (B and C) Stereological quantification of the number of CD4-positive cells in the SN in (B) placebo or (C) FK506 (1 mg/kg)-treated animals over time (mean ± SD, $^*p < 0.05$ by ANOVA and Tukey post hoc test, $\#p < 0.05$ vs. the other group at same time point, n = 3–4). (D) IHC staining for CD8 on placebo-treated animals 15 days after rAAV α-synuclein injection. Scale bar = 30 μm. (E) Stereological quantification of the number of CD8-positive cells in the SN in (E) placebo or (F) FK506 (1 mg/kg)-treated animals over time (mean ± SD, $^*p < 0.05$ by ANOVA and Tukey post hoc test, $\#p < 0.05$ vs. the other group at same time point, n = 4). Abbreviations: ANOVA, analysis of variance; SD, standard deviation; SN, substantia nigra.

window of FK506 in A53T α-synuclein rAAV–injected rats. In addition, the observed wide range in trough FK506 concentration ratios between blood and CSF, suggests an important variability in penetration of FK506 into the rat brain which is at least partially determined by P-glycoprotein activity in the blood brain barrier (Yokogawa et al., 1999).

In an attempt to elucidate the mechanism by which FK506 prevents α-synuclein–induced degeneration, we first investigated whether FK506 affects α-synuclein aggregation in the brain. Our group was the first to make a direct link between FKBP12 and α-synuclein aggregation in vitro and in cell culture (Deleersnijder et al., 2011; Gerard et al., 2008, 2010). We also showed that administration of FK506 reduces α-synuclein aggregation and cell death after LV α-synuclein delivery into mouse striatum (Gerard et al., 2010). However, in this rAAV2/7 based α-synuclein rat model, we could not detect a significant effect of FK506 on α-synuclein aggregation. This may be explained by the fact that the aggregation kinetics in our rat model are considerably faster than in the previously used LV mouse model, because of the higher expression levels combined with the use of the aggregation-prone A53T mutant of α-synuclein. Furthermore, because of a higher sensitivity of the dopaminergic neurons of the SN, the extent of neuronal degeneration in our rat model is also significantly higher compared with the degeneration in the mouse striatum. Future experiments using FK506 with a lower dose of rAAV2/7 vector might reveal a potentially more subtle and slower additional effect on α-synuclein aggregation. Furthermore, the development of new methods and tools to distinguish between different α-synuclein species would allow a more refined analysis.

As FK506 also exhibits strong immunosuppressive effects, it may exert its neuroprotective effect by affecting the microglia and macrophage population through the adaptive immune response. Neuroinflammation and adaptive immunity have frequently been linked to neurodegeneration including PD, although the causal relationship is still under debate (Mosley et al., 2012). Microglia activation and neuroinflammation have been described in various α-synuclein models, but the therapeutic relevance has not yet been demonstrated (Gao et al., 2011; Su et al., 2008, 2009; Theodore et al., 2008). Microglia activation profiles observed in our rat model are in line with previous findings (Sanchez-Guajardo et al., 2010), except for some small differences probably because of the degree of neurodegeneration. Overexpression of α-synuclein by means of rAAV2/7 induced an increase in the number of Mac1-positive microglia and macrophages and phagocytic (CD68+) macrophages, but also influenced the humoral immune response, as both antigen presenting macrophages (MHC II+) as well as T helper cells (CD4+) and cytotoxic T cells (CD8+) were elevated in α-synuclein overexpressing rats. Furthermore, in the presence of high levels of dopaminergic neurodegeneration, microglia showed a predominant clustered macrophagic morphology (type C) which correlates with elevated CD68+ expression (phagocytic marker). Although we cannot prove a direct causal relationship, the presence of type C microglial cells correlated well with conditions of the highest dopaminergic cell death. Treatment with FK506 did not induce detectable changes in the number of CD68+ and MHC II+ macrophages but reduced the number of Mac1+ microglia and macrophages. Moreover, a different pattern of microglia morphology was observed in the FK506 group compared with the placebo group. Treatment of FK506 decreased the number of "clustered microglia". This is in line with previous studies showing that FK506 can suppress the activation of these proinflammatory macrophages (Yoshino et al., 2010).

In addition, FK506-treated animals presented a lower number of CD4+ T helper cells 29 days p.i. and a delayed infiltration of cytotoxic T cells 15 days p.i. These findings could be explained by the direct anti-proliferative effect of FK506 on CD4 or CD8+ T cells (Jones et al., 2006), as well as by the reduced number of microglia (Zawadzka and Kaminska, 2005), leading to lowered chemokine secretion and a reduced attractive environment for CD4 and CD8+ T cells. Our findings suggest that FK506 ameliorates DN survival by lowering the infiltration of T cells and the number of Mac1+ microglia and macrophages, but without any effect on classically activated (CD68+) macrophages or α-synuclein aggregation. Similarly, FK506 has also been shown to mediate neuroprotection through its anti-inflammatory effects in animal models of tauopathy (Yoshiyama et al., 2007).

In summary, we have shown that FK506 provides neuroprotection in a robust A53T α-synuclein rAAV2/7–based rat model, thereby linking neuroinflammation to early progression of synucleinopathy. Because FK506 (tacrolimus) has been administered to kidney transplant patients for a long time, it would be worthwhile to perform meta-analysis studies on the chronic use of tacrolimus and the incidence of PD. Our data support further efforts for pharmacologic modulation of neuroinflammation in Parkinson's disease.

Disclosure statement

The authors declare that there is no actual or potential conflict of interest.

Acknowledgements

The authors thank Joris Van Asselberghs and Caroline van Heijningen (KU Leuven), Drs Marijn Van Hulle and Kristof Pil (Waters Company Belgium) for their excellent technical assistance. Research was funded by the IWT-Vlaanderen (IWT SBO/80020), the FWO Vlaanderen (G.0768.10), by the EC-FP6 program "DiMI" (LSHB-CT-2005–512146), the FP7 RTD project MEFOPA (HEALTH-2009–241791), the FP7 program "INMiND" (HEALTH-F2-2011–278850), the KU Leuven (IOF-KP/07/001, OT/08/052A, IMIR PF/10/017), and the MJFox Foundation (Target validation 2010).

Appendix A. Supplementary data

Supplementary data associated with this article can be found, in the online version, at http://dx.doi.org/10.1016/j.neurobiolaging.2015.01.014.

References

Baekelandt, V., Claeys, A., Eggermont, K., Lauwers, E., De Strooper, B., Nuttin, B., Debyser, Z., 2002. Characterization of lentiviral vector-mediated gene transfer in adult mouse brain. Hum. Gene Ther. 13, 841–853.

Braak, H., Sastre, M., Del Tredici, K., 2007. Development of alpha-synuclein immunoreactive astrocytes in the forebrain parallels stages of intraneuronal pathology in sporadic Parkinson's disease. Acta Neuropathol. 114, 231–241.

de Jonge, H., de Loor, H., Verbeke, K., Vanrenterghem, Y., Kuypers, D.R., 2012. In vivo CYP3A4 activity, CYP3A5 genotype, and hematocrit predict tacrolimus dose requirements and clearance in renal transplant patients. Clin. Pharmacol. Ther. 92, 366–375.

Deleersnijder, A., Van Rompuy, A.S., Desender, L., Pottel, H., Buee, L., Debyser, Z., Baekelandt, V., Gerard, M., 2011. Comparative analysis of different peptidyl-prolyl isomerases reveals FK506-binding protein 12 as the most potent enhancer of alpha-synuclein aggregation. J. Biol. Chem. 286, 26687–26701.

Deroose, C.M., Reumers, V., Gijsbers, R., Bormans, G., Debyser, Z., Mortelmans, L., Baekelandt, V., 2006. Noninvasive monitoring of long-term lentiviral vector-mediated gene expression in rodent brain with bioluminescence imaging. Mol. Ther. 14, 423–431.

Gao, H.M., Zhang, F., Zhou, H., Kam, W., Wilson, B., Hong, J.S., 2011. Neuroinflammation and alpha-synuclein dysfunction potentiate each other, driving chronic progression of neurodegeneration in a mouse model of Parkinson's disease. Environ. Health Perspect. 119, 807–814.

Gerard, M., Debyser, Z., Desender, L., Baert, J., Brandt, I., Baekelandt, V., Engelborghs, Y., 2008. FK506 binding protein 12 differentially accelerates fibril formation of wild type alpha-synuclein and its clinical mutants A30P or A53T. J. Neurochem. 106, 121–133.

Gerard, M., Deleersnijder, A., Daniels, V., Schreurs, S., Munck, S., Reumers, V., Pottel, H., Engelborghs, Y., Van den Haute, C., Taymans, J.M., Debyser, Z., Baekelandt, V., 2010. Inhibition of FK506 binding proteins reduces alpha-synuclein aggregation and Parkinson's disease-like pathology. J. Neurosci. 30, 2454–2463.

Gold, B.G., Nutt, J.G., 2002. Neuroimmunophilin ligands in the treatment of Parkinson's disease. Curr. Opin. Pharmacol. 2, 82–86.

Iwasaki, K., 2007. Metabolism of tacrolimus (FK506) and recent topics in clinical pharmacokinetics. Drug Metab. Pharmacokinet. 22, 328–335.

Jones, D.L., Sacks, S.H., Wong, W., 2006. Controlling the generation and function of human CD8+ memory T cells in vitro with immunosuppressants. Transplantation 82, 1352–1361.

Kaminska, B., Gaweda-Walerych, K., Zawadzka, M., 2004. Molecular mechanisms of neuroprotective action of immunosuppressants–facts and hypotheses. J. Cell Mol. Med. 8, 45–58.

Kitamura, Y., Itano, Y., Kubo, T., Nomura, Y., 1994. Suppressive effect of FK-506, a novel immunosuppressant, against MPTP-induced dopamine depletion in the striatum of young C57BL/6 mice. J. Neuroimmunol. 50, 221–224.

Liu, J., Albers, M.W., Wandless, T.J., Luan, S., Alberg, D.G., Belshaw, P.J., Cohen, P., MacKintosh, C., Klee, C.B., Schreiber, S.L., 1992. Inhibition of T cell signaling by immunophilin-ligand complexes correlates with loss of calcineurin phosphatase activity. Biochemistry 31, 3896–3901.

Liu, J., Farmer Jr., J.D., Lane, W.S., Friedman, J., Weissman, I., Schreiber, S.L., 1991. Calcineurin is a common target of cyclophilin-cyclosporin A and FKBP-FK506 complexes. Cell 66, 807–815.

Ma, S.Y., Roytta, M., Rinne, J.O., Collan, Y., Rinne, U.K., 1997. Correlation between neuromorphometry in the substantia nigra and clinical features in Parkinson's disease using disector counts. J. Neurol. Sci. 151, 83–87.

Mosley, R.L., Hutter-Saunders, J.A., Stone, D.K., Gendelman, H.E., 2012. Inflammation and adaptive immunity in Parkinson's disease. Cold Spring Harb. Perspect. Med. 2, a009381.

Napoli, K.L., Hammett-Stabler, C., Taylor, P.J., Lowe, W., Franklin, M.E., Morris, M.R., Cooper, D.P., 2010. Multi-center evaluation of a commercial kit for tacrolimus determination by LC/MS/MS. Clin. Biochem. 43, 910–920.

Poulter, M.O., Payne, K.B., Steiner, J.P., 2004. Neuroimmunophilins: a novel drug therapy for the reversal of neurodegenerative disease? Neuroscience 128, 1–6.

Sanchez-Guajardo, V., Febbraro, F., Kirik, D., Romero-Ramos, M., 2010. Microglia acquire distinct activation profiles depending on the degree of alpha-synuclein neuropathology in a rAAV based model of Parkinson's disease. PLoS One 5, e8784.

Schmitz, C., Hof, P.R., 2005. Design-based stereology in neuroscience. Neuroscience 130, 813–831.

Su, X., Federoff, H.J., Maguire-Zeiss, K.A., 2009. Mutant alpha-synuclein overexpression mediates early proinflammatory activity. Neurotox Res. 16, 238–254.

Su, X., Maguire-Zeiss, K.A., Giuliano, R., Prifti, L., Venkatesh, K., Federoff, H.J., 2008. Synuclein activates microglia in a model of Parkinson's disease. Neurobiol. Aging 29, 1690–1701.

Theodore, S., Cao, S., McLean, P.J., Standaert, D.G., 2008. Targeted overexpression of human alpha-synuclein triggers microglial activation and an adaptive immune response in a mouse model of Parkinson disease. J. Neuropathol. Exp. Neurol. 67, 1149–1158.

Van der Perren, A., Toelen, J., Carlon, M., Van den Haute, C., Coun, F., Heeman, B., Reumers, V., Vandenberghe, L.H., Wilson, J.M., Debyser, Z., Baekelandt, V., 2011. Efficient and stable transduction of dopaminergic neurons in rat substantia nigra by rAAV 2/1, 2/2, 2/5, 2/6.2, 2/7, 2/8 and 2/9. Gene Ther. 18, 517–527.

Van der Perren, A., Toelen, J., Casteels, C., Macchi, F., Van Rompuy, A.S., Sarre, S., Casadei N., Nuber S., Himmelreich U., Osorio Garcia M.I., Michotte Y., D'Hooge R., Bormans G., Van Laere K., Gijsbers R., Van den Haute C., Debyser Z. and Baekelandt V., 2014. Longitudinal characterization of a robust rat model for Parkinson's disease based on overexpression of alpha-synuclein with rAAV2/7 viral vectors. Neurobiol. Aging 36, 1543–1558.

Wright, A.K., Miller, C., Williams, M., Arbuthnott, G., 2008. Microglial activation is not prevented by tacrolimus but dopamine neuron damage is reduced in a rat model of Parkinson's disease progression. Brain Res. 1216, 78–86.

Yokogawa, K., Takahashi, M., Tamai, I., Konishi, H., Nomura, M., Moritani, S., Miyamoto, K., Tsuji, A., 1999. P-glycoprotein-dependent disposition kinetics of tacrolimus: studies in mdr1a knockout mice. Pharm. Res. 16, 1213–1218.

Yoshino, T., Nakase, H., Honzawa, Y., Matsumura, K., Yamamoto, S., Takeda, Y., Ueno, S., Uza, N., Masuda, S., Inui, K., Chiba, T., 2010. Immunosuppressive effects of tacrolimus on macrophages ameliorate experimental colitis. Inflamm. Bowel Dis. 16, 2022–2033.

Yoshiyama, Y., Higuchi, M., Zhang, B., Huang, S.M., Iwata, N., Saido, T.C., Maeda, J., Suhara, T., Trojanowski, J.Q., Lee, V.M., 2007. Synapse loss and microglial activation precede tangles in a P301S tauopathy mouse model. Neuron 53, 337–351.

Zawadzka, M., Kaminska, B., 2005. A novel mechanism of FK506-mediated neuroprotection: downregulation of cytokine expression in glial cells. Glia 49, 36–51.